



Applications of spectroscopic methods in studies of polyoxometalates and their complexes with lanthanide(III) ions

Stefan Lis

Department of Rare Earths, Faculty of Chemistry, Adam Mickiewicz University, Grunwaldzka 6, 60-780 Poznan, Poland

Abstract

Polyoxometalates (POMs), due to their attractive physical and chemical properties, biological significance as well as wide applications, have been the subject of numerous studies. The results of investigations concerning the synthesis, properties and structure of POMs and their lanthanide(III) complexes (LnPOM) are briefly reviewed. Useful techniques for the verification of POM compositions and the determination of components, including new spectrophotometric methods for the determination of tungsten and molybdenum and for simultaneous determination of these elements in structures of POMs and their LnPOM complexes, are described. The important role of the Nd(III) hypersensitive absorption band and Eu(III) luminescence spectroscopy as well as FTIR spectra in the investigation of POMs and LnPOM complexes is discussed. The use of EPR to study magnetic properties and coordination of Gd(III) complexes with POMs, and to probe the local environment of the host metal site in terms of symmetry, is presented. © 2000 Elsevier Science S.A. All rights reserved.

Keywords: Polyoxometalates; Lanthanide(III) complexes; Absorption and luminescence spectroscopy; EPR

1. Introduction

The early transition metals (V, Nb, Ta, Mo, W) in their highest oxidation states are able to form metal oxygen cluster anions, commonly referred to as polyoxometalates (POMs) [1]. The chemistry of POM anions, an important subarea of modern inorganic chemistry, is dominated by molybdenum and tungsten in their +6 oxidation state. During the last two decades this class of compounds has received much attention because of their interesting properties, importance as reagents in analytical procedures and wide applications in catalysis, biology, material science and medicine as inorganic drugs [1–4]. The coordination chemistry of polyoxoanions is today one of the most active areas in polyoxometalate chemistry. The investigation of POM complexes with metal ions, including Ln(III) ions, has important significance due to their antiviral and anti-HIV activity and potential applications as imaging contrast agents [3,4]. POMs form a unique class of compounds with high symmetry [5]. These discrete polyanions are water-soluble structures with charges ranging from –3 to –14.

2. Structure and synthesis

The majority of POMs are composed of structures constructed from molybdenum and tungsten polyhedrons.

Although new structural types of polyanions continue to be discovered, it is possible to recognize some general principles that control such structures. A very large number of POMs are viewed as arrangements of edge- and vertex-sharing MO_6 octahedra, each with one or two unshared vertices (terminal oxygens) [6]. The polyanion surfaces are therefore bounded by weakly or non-basic multiply bounded oxygen atoms, and discourage any further polymerization. The majority of POM structures have been categorized into three structural groups [7]. Groups 1 and 2 are characterized by a highly symmetrical assembly of MO_6 octahedra [most commonly, $\text{M}=\text{Mo(VI)}$, W(VI) ; also $\text{M}=\text{V(V)}$, Nb(V) and Ta(V)] which surround a central core. For Group 1 structures (e.g., $\text{SiW}_{12}\text{O}_{40}^{4-}$, $\text{P}_2\text{W}_{18}\text{O}_{62}^{6-}$), the core is composed of one or two XO_4 tetrahedra [where the heteroelement $\text{X}=\text{B(III)}$, P(III) , Si(IV) , Ge(IV)], whereas for Group 2 structures (e.g., $\text{MnMo}_9\text{O}_{32}^{6-}$), the central core is a transition metal octahedron XO_6 [e.g., $\text{X}=\text{Mo(VI)}$, Mn(II)]. Group 3 structures (e.g., $\text{CeO}_{12}\text{O}_{42}^{8-}$) are based on an icosahedrally coordinated central core. Among the many heteropolytungstate anions there are three compositions: $[(\text{Na})\text{P}_5\text{W}_{30}\text{O}_{110}]^{14-}$, $[(\text{Na})\text{Sb}_9\text{W}_{21}\text{O}_{86}]^{18-}$ and $[(\text{K})\text{As}_4\text{W}_{40}\text{O}_{140}]^{27-}$ which function as inorganic cryptands. They can encapsulate alkali metal cations and lanthanide ions selectively [8–10].

The spherical-like structures of Group 1 are called

plenary structures (latin *plenarius* full, complete), and their degraded derivatives are called *lacunary* structures (latin *lacunar* gap, pit). The *plenary* structures are further categorized by the number of central tetrahedra, where the Keggin structure ($\text{XM}_{12}\text{O}_{40}^{n-}$) and the Dawson structure ($\text{X}_2\text{M}_{18}\text{O}_{62}^{m-}$) have one and two central tetrahedra, respectively. Synthesis of POMs occurs by a remarkable self-assembly process governed by the reaction conditions, notably pH, ratio of reactants, and temperature. The general formation process is the condensation of monomeric oxometalates (i.e. WO_4^{2-} or MoO_4^{2-} and PO_4^{2-} , AsO_2^- , Sb_2O_3 , etc.) in acidic aqueous solution. Under such conditions, protons function as oxygen abstractors in a dehydration process [1], due to the beneficial combination of ionic radius, charge and accessibility of d-orbitals for metal–oxygen π -bonding [11]. Other researchers have suggested that the dehydration process accounts for a very favorable entropy change with the formation of more compact structures [7] or, alternatively, have made a more quantitative attempt to rationalize the existence and stability of the various structures based on the number of closed loops of $-\text{O}-\text{M}-\text{O}-\text{M}-\text{O}-$ linkages, such as in a triad [12], with π -bonding character in $\text{M}-\text{O}-\text{M}$ bridges [13]. Since the molybdenum or tungsten atoms are in their highest oxidation state (+6), there are no electrons available for metal–metal binding and the structures are held together by metal–oxygen bonds [14].

3. Characterization

The polyoxometalates may be characterized by six features: (1) an electrochemical or photochemical reversible multi-electron redox reaction, (2) high solubility in water and occasionally in polar organic solvents, (3) coordination of a large number of water molecules, (4) facility of the modification of anion size, structure, anion charge and replacement of metal atoms by other metal atoms, (5) coordination of a great variety of hetero atoms, with as many as 75% of the elements in the Periodic Table occupying well-defined geometric sites in the lattice, and (6) encapsulation of neutral molecules (acetonitrile) or ions (carbonate or halide) [15].

Due to the potential difficulties with chemical analysis, POM composition is best verified using several techniques. A useful method must have the accuracy to distinguish between very similar formulations (e.g., such as $\text{P}_2\text{W}_{17}\text{O}_{61}^{10-}$ and $\text{P}_2\text{W}_{18}\text{O}_{62}^{6-}$) and the precision to determine the heteroelements which are in low abundance (<1 to 2%) [16]. Polarographic techniques have proven useful for the determination of molybdenum and tungsten in POMs [17,18], however the central heteroelement concentrations are typically measured by laborious, time-consuming gravimetric, titrimetric or colorimetric procedures [1]. Polarography and cyclic voltammetry are useful for “fin-

gerprint” characterization, especially in differentiating between isomers [16]. With the availability of higher resolution spectrometers, inductively coupled plasma-atomic emission spectroscopy (ICP-AES) can be considered as a practical tool for POM analysis, however limitations of this technique are associated with potential element interferences [19]. Raman spectroscopy in H_2O [20] and IR spectroscopy in D_2O [12] have been used to fingerprint the polyanion structures in solutions. Correlations between spectral peak positions, shapes, and relative intensities between solid state and solution spectra strongly suggest identical structures [1]. Studies using ^{183}W NMR are valuable to elucidate the defect nature of the *lacunary* structure of POMs [21].

The determination of Mo and W is more complicated than for the central heteroelements. We have proposed two new spectrophotometric methods for the determination of tungsten and molybdenum or the simultaneous determination of these elements in structures of POMs and their LnPOM complexes [22,23].

One of the methods is based on the use of disodium-1,2-dihydrobenzene-3,5-disulfate (Tiron) as a colorimetric reagent [22]. Contents of Mo(VI) and W(VI) in solutions of polyoxotungstates and polyoxomolybdates can be determined by measuring absorbances as a function of concentration from the wavelength range 352–500 nm for molybdenum and 352–400 nm for tungsten, where Beer’s law is obeyed. This method can also be applied for the simultaneous determination of these elements, without previous chemical separation, in polyoxotungstomolybdates. The procedure is based on the measurement of absorption spectra using values of the absorbance. The content of Mo and W is determined from from the molar absorptivity coefficients for Mo and W ions at two points in the absorption spectrum. The method allows the determination of Mo(VI) in the concentration range 2–10 $\mu\text{g}/\text{ml}$ and W(VI) at 4–20 $\mu\text{g}/\text{ml}$, and also enables the determination of Mo(VI) and W(VI) in the presence of other elements which occur in the structures of polyoxometalates and their complexes. This method was also satisfactorily applied for the determination of Mo(VI) and W(VI) in polyoxometalate complexes with Ln(III) ions. The presence of Ln(III), occurring in excess as interfering ions in measured systems, does not interfere in the determination of Mo(VI) and W(VI) in Ln/POM complexes.

The second procedure for the spectrophotometric determination of tungsten in POMs [23] is based on a preliminary extraction with oxine–chloroform, from hydrofluoric acid solution, to remove impurities interfering in W determination. After addition of boric acid and adjustment of the pH to 2.0, W is extracted. An excess of oxine and interfering metal oxine complexes are washed from the chloroform phase with ammonium sulfate–sulfuric acid solution. The chloroform extract is used for tungsten spectrophotometric determination. Tungsten absorption at

358 nm is measured against chloroform as a reference. The dependence of tungsten absorbance on its concentration is linear from 5 to 35 mg/ml. The tungsten concentrations obtained by spectrophotometric determination of heteropolyanions and their europium derivatives (sandwiched and encrypted) were very satisfactory. Both methods have sufficient accuracy to distinguish between very similar formulations and the sensitivity to determine elements which are in low abundance. The value of the standard error was <4% and the linear regression coefficients $r^2 > 0.999$.

4. Spectroscopic studies of complexes with lanthanide ions

Polyoxometalates can bind metal cations via surface terminal and bridging oxygens (e.g., *plenary* structures) or by enclosing them in a defect site (e.g., *lacunary* structures) [11]. In the first type of complex, monodentate ligands bind metal ions such as Mn(II) or Eu(III) through a single terminal oxygen and the complexes are weak and labile. There are numerous examples of the second type, which occur through the four exterior oxygens that define the defect site of *lacunary* derivatives [11]. Transition metals are small enough to be enclosed in the vacant site and are isolated as 1:1 complexes, with solvent molecules completing the coordination sphere (e.g., $[(\text{SiW}_{11}\text{O}_{39})\text{Co}(\text{H}_2\text{O})]^{6-}$). However, lanthanide ions, with their larger ionic radii and higher charge densities, have been isolated as the Ln(POM)₂ complexes in which the lanthanide is sandwiched between the defect site of two ligands.

Lanthanide ion absorption (in the UV–visible and the near-IR region) and luminescence are characterized by narrow bands which are ascribed to internal transitions within the 4f shell (i.e., f→f transitions) [24] and, since $\Delta l = 0$, are Laporte forbidden. Therefore, f→f transitions are weaker and sharper than d→d transitions and the ligand field effect is considerably smaller. Ln(III) absorption and luminescence spectra have proven useful for characterization of Ln/POM complexes in solution and the solid state.

4.1. Absorption spectra of hypersensitive transitions

Hypersensitive transitions (f→f transitions in which the absorption maximum and intensity are sensitive to the ligand field) can be used to evaluate the binding site, stoichiometry and site symmetry of Ln/POM complexes. However, due to the weak nature of f→f transitions, the sensitivity of absorption measurements is limited. The absorption bands in a range of hypersensitive transitions allow evaluation of the formation of Nd/POM complexes. We used the absorption spectra of Nd(III) (the transition ${}^4\text{I}_{9/2} \rightarrow {}^4\text{F}_{5/2}$ at $\lambda_{\text{max}} \sim 796$ nm) for spectroscopic characterization of a series of Nd(III): sandwiched $[\text{Nd}(\text{POM})_2]$, encapsulated within the cavity of the POM, and 2:1-type (Nd₂POM) complexes [25]. The spectra were measured for various Nd(III)/POM ratios and as a function of ionic strength. For instance, absorption spectra of Nd(III) with lacunary POMs have shown the formation of the sandwiched complex Nd(POM)₂ or the 2:1-type (Ln₂MnMo₉O₃₂) complex with the $[\text{MnMo}_9\text{O}_{32}]^{6-}$ ligand [25]. Based on the Nd(III) absorption spectra, the values of the oscillator strength, P , for several studied complexes were calculated as described in Ref. [26]. The P values obtained for the Nd(III) ${}^4\text{I}_{9/2} \rightarrow {}^4\text{F}_{5/2}$ transition (in the range 775–830 nm) in aqueous solutions of several NdPOM complexes for various POM/Nd(III) molar ratios (Table 1) confirm the formation of particular types of Ln/POM complexes.

4.2. Eu(III) luminescence spectroscopy

Some members of the lanthanide series have excited states which relax by emission of photons. While such electronic transitions within a 4fⁿ configuration are still Laporte forbidden, an intense laser beam can be used as an excitation source to access the excited state and monitor its luminescence decay quantitatively even in dilute solutions. Laser-induced lanthanide ion luminescence has been used in complexation studies for various systems. The excited state lifetime is efficiently quenched by O–H oscillators of inner sphere H₂O molecules bound to the Eu(III) ion. The difference in the decay rate of the excited state in H₂O and D₂O is proportional to the number, n , of water molecules

Table 1

Values of the oscillator strength, $P \times 10^6$, calculated for the Nd(III) ${}^4\text{I}_{9/2} \rightarrow {}^4\text{F}_{5/2}$ transition (in the range 775–830 nm) in aqueous solutions of several NdPOM complexes for various POM/Nd(III) molar ratios

Polyoxometalate anion	Oscillator strength ($P \times 10^6$) POM/Nd(III) ratio								
	0	0.2	0.5	0.8	1	1.5	2	3	
$[\text{SiW}_{11}\text{O}_{39}]^{8-}$	8.27		10.88	12.54		13.50	13.98	12.23	
$[\text{PW}_{11}\text{O}_{39}]^{7-}$	8.27		9.42		10.76	10.93	11.32	11.03	
$[\text{MnMo}_9\text{O}_{32}]^{6-}$	8.27	9.07	9.60	10.21	10.49				
$[\text{NiMo}_9\text{O}_{32}]^{6-}$	8.27	8.95	9.52		10.51				
$[(\text{Na})\text{As}_4\text{W}_{40}\text{O}_{140}]^{27-}$	8.27	10.26	10.78	11.88	12.19		12.16		

in the first coordination sphere as described by the equations [27,28]

$$n_{\text{H}_2\text{O}} = 1.05(\tau_{\text{H}_2\text{O}}^{-1} - \tau_{\text{D}_2\text{O}}^{-1}) \quad (1)$$

$$n_{\text{H}_2\text{O}} = 1.05\tau_{\text{H}_2\text{O}}^{-1} - 0.7 \quad (2)$$

where $\tau_{\text{H}_2\text{O}}^{-1} = k(\text{H}_2\text{O})$ and $\tau_{\text{D}_2\text{O}}^{-1} = k(\text{D}_2\text{O})$ are exponential decay constants for the luminescence intensity (reciprocal measured lifetime) of the excited state of Eu(III) in H_2O and D_2O , respectively. The uncertainty has been estimated as ± 0.5 H_2O molecules.

Using this technique we have studied representative POMs, categorized into three structural groups, having tetrahedrally, octahedrally and icosahedrally coordinated central cores, and compositions that encapsulate lanthanides [25,29,30]. Data from a series of Eu(III) complexes forming sandwiched $\text{Eu}(\text{POM})_2$, Eu_2POM , and encapsulated (within the cavity of the POM) complexes are presented together with luminescence data in Table 2.

Eu(III) luminescence lifetimes, measured both for solid and aqueous (H_2O and D_2O) solutions, indicate that the sandwiched complexes have no water of hydration, whereas europium-encrypted derivatives have three (solid) or four (solution) water molecules and the $\text{Eu}/\text{POM}=2:1$ complexes have four to six water molecules in the Eu(III) inner coordination sphere. In the case of the europium-encrypted Preyssler polyanion $[\text{EuP}_5\text{W}_{30}\text{O}_{110}]^{12-}$ we found three water molecules in the inner sphere of the europium-encapsulated complex, both in aqueous solution and in the solid state [23].

The Eu(III) luminescence spectrum shows two intense bands at 594 and 615 nm, associated with $^5\text{D}_0 \rightarrow ^7\text{F}_1$ and $^5\text{D}_0 \rightarrow ^7\text{F}_2$ (exhibiting hypersensitivity) transitions, and their relative intensities (ratio $\eta = I_{615}/I_{594}$) are sensitive to the primary coordination sphere about the Eu(III) ion. Calculated values of η are presented in Table 2, together

with Eu(III) luminescence lifetimes and hydration numbers of the complexes studied. The highest symmetry (lowest η values) of the Eu(III) ion was observed in the case of complexes $[(\text{Eu})\text{P}_5\text{W}_{30}\text{O}_{110}]^{12-}$ and $[\text{Eu}(\text{SiW}_{11-x}\text{Mo}_x\text{O}_{39})_2]^{13-}$. The η values (Table 2) indicate that a higher symmetry is observed for the EuPOM complexes in the solid state than in aqueous solution.

The most intense Eu(III) luminescence was observed for the $(\text{EuW}_{10}\text{O}_{36})^{9-}$ and $[\text{Eu}(\text{SiW}_{10}\text{MoO}_{39})_2]^{13-}$ sandwiched complexes and for $(\text{Eu}_2\text{CeMo}_{12}\text{O}_{42})^{6-}$ due to energy transfer from the tungstate group to the Eu(III) ion [29,31]. The luminescence excitation spectra show the intense broad bands of the oxygen-to-metal charge transfer (O–M) LMCT (with max. 250–360 nm). The $(\text{EuW}_{10}\text{O}_{36})^{9-}$ and $[\text{Eu}(\text{SiW}_{10}\text{MoO}_{39})_2]^{13-}$ complexes have potential in analytical applications by spectrofluorimetry. In the case of $[\text{Eu}(\text{SiW}_{11}\text{O}_{39})_2]^{13-}$ and $[\text{Eu}(\text{PW}_{17}\text{O}_{61})_2]^{17-}$ and the Eu-encrypted complexes, a weak luminescence intensity is observed. In these cases the charge transfer from ligand to Eu(III) does not occur. The I_{lum} of Eu(III) in Eu/POM complexes in aqueous solution depends on the ionic strength. The I_{lum} increases as I increases. The Eu(III) luminescence intensity of tungstomolybdate sandwiched complexes indicates a decrease in the efficiency of the energy transfer from the polytungstate group to Eu(III) in $[\text{Eu}(\text{SiW}_{11-x}\text{Mo}_x\text{O}_{39})_2]^{13-}$ polyanions as x increases.

An interesting pattern of Eu(III) luminescence intensity and lifetime was observed in the case of the heterotungstomolybdate sandwich complexes [29]. A linear dependence of the luminescence lifetime, τ , of the Eu(III) ion on the content of Mo (number of atoms, $x = 0-9$) in the $[\text{Eu}(\text{SiW}_{11-x}\text{Mo}_x\text{O}_{39})_2]^{13-}$ structure was observed, most probably due to the differences in the ionic radii of W(VI) and Mo(VI) ions. The correlation gave the following equations for the calculation of the number, x , of Mo atoms in each structure:

Table 2

Luminescence data and hydration numbers of Eu/POM (sandwiched, encrypted and 2:1) complexes in solid and aqueous solution^a

POM composition	Solution		Solid				
		τ (ms)	$n_{\text{H}_2\text{O}}$	η	$\tau_{\text{H}_2\text{O}}$ (ms)	$\tau_{\text{D}_2\text{O}}$ (ms)	$n_{\text{H}_2\text{O}}$
$[\text{EuW}_{10}\text{O}_{36}]^{9-}$	1.0	2.43	0	0.4	2.29	4.42	0
$[\text{Eu}(\text{SiW}_{11}\text{O}_{39})_2]^{8-}$	0.8	2.43	0	1.0	3.46	5.38	0
$[\text{Eu}(\text{P}_2\text{W}_{17}\text{O}_{61})_2]^{17-}$	1.2	2.13	0	1.8	3.08	4.76	0
$[\text{Eu}(\text{SiMo}_2\text{W}_9\text{O}_{39})_2]^{13-}$	1.0	2.08	0	1.3	3.21	4.83	0
$\text{Eu}_2\text{TeMo}_6\text{O}_{24}$	3.9	0.19 (H_2O) 1.15 (D_2O)	4	4.1	0.16	1.20	6
$[\text{Eu}_2\text{CeMo}_{12}\text{O}_{42}]^{2-}$	–	0.21 (H_2O) 0.96 (D_2O)	4	2.9	0.22	–	4
$[\text{EuP}_5\text{W}_{30}\text{O}_{110}]^{12-}$	–	0.30 (H_2O) 2.52 (D_2O)	3	1.1	0.32	5.03	3
$[\text{EuAs}_4\text{W}_{40}\text{O}_{140}]^{25-}$	3.9	0.26	3	4.3	0.25	2.21	4
$[\text{EuSb}_9\text{W}_{21}\text{O}_{86}]^{16-}$	5.4	0.27	3	–	0.22	1.35	4

^a $\eta = I_{615}/I_{594}$ is the ratio of Eu(III) luminescence intensity bands at 594 and 615 nm; τ is the Eu(III) luminescence lifetime; $n_{\text{H}_2\text{O}}$ is the hydration number of Eu(III) complexes.

$$x_{\text{Mo}} = (2.362 - \tau)/0.096 \text{ in the solid}$$

$$x_{\text{Mo}} = (3.392 - \tau)/0.127 \text{ in H}_2\text{O, and}$$

$$x_{\text{Mo}} = (5.539 - \tau)/0.287 \text{ in D}_2\text{O solution}$$

where τ is the Eu(III) luminescence lifetime in milliseconds

Similarly, a linear dependence of the Eu(III) luminescence quantum yield, ϕ , on the number of Mo atoms, x , in these structures was obtained [30]. The relationship of ϕ to x is described by the following equation for the calculation of the number of Mo atoms, x , in Eu(III)/tungstomolybdate structures:

$$x_{\text{Mo}} = -(1.9477 + \log \phi)/0.2469$$

where ϕ is the Eu(III) luminescence quantum yield.

These dependencies can be applied to the determination of the Mo content of polytungstomolybdate complexes. The least-squares fit of the data had correlation coefficients of 0.999 in all cases for τ measurements and 0.997 for the ϕ dependence.

4.3. IR spectroscopy

IR spectroscopy has been used to fingerprint the polyanion structures in solution. Correlations between spectral peak positions, shapes, and relative intensities between solid state and solution spectra strongly suggest identical structures [1]. The FTIR spectra of heteropolytungstate systems show distinctive differences between plenary and lacunary structures as well as their complexes with Ln(III), as shown in Fig. 1.

Characterization of POMs utilizes IR absorption spectra ($1500\text{--}200 \text{ cm}^{-1}$). The FTIR spectra recorded for heteropolytungstates and Ln(III) sandwiched or encrypted complexes have four regions which correspond to metal–oxygen oscillations: $900\text{--}600 \text{ cm}^{-1}$ (W–O–W bending), $1000\text{--}900 \text{ cm}^{-1}$ (W–O stretching), $1200\text{--}1000 \text{ cm}^{-1}$ (P–O, Si–O ionic stretching), and an O–H oscillation region

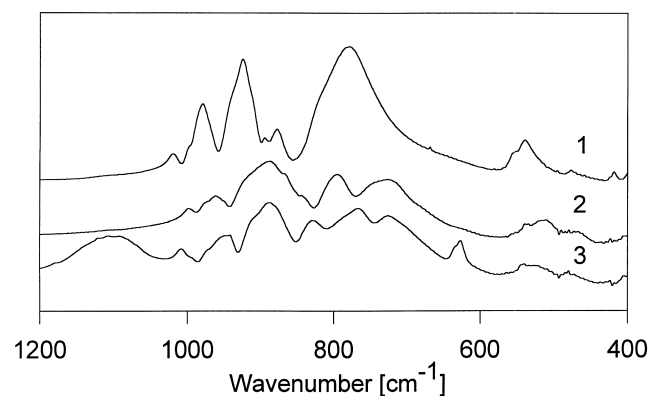


Fig. 1. FTIR spectra of $(\text{SiW}_{12}\text{O}_{40})^{4-}$ plenary (1) and $(\text{SiW}_{11}\text{O}_{39})^{8-}$ lacunary (2) anions, and the $[\text{Eu}(\text{SiW}_{11}\text{O}_{39})_2]^{13-}$ sandwiched complex (3).

with two maxima, at $\sim 3650 \text{ cm}^{-1}$ (stretching) and 1610 cm^{-1} (bending). The latter O–H region indicates water of crystallization. Tungstophosphates exhibit P–O absorption bands at $1200\text{--}1000 \text{ cm}^{-1}$, separated from the W–O absorption region ($<950 \text{ cm}^{-1}$), while for tungstoarsenates, the corresponding As–O bands at $910\text{--}950 \text{ cm}^{-1}$ are overlapped by W–O absorptions [32]. The FTIR spectra exhibit shifts of characteristic bands, indicating an effect of the rigidity of POM systems. Data for the FTIR spectra of the compounds studied are collected in Table 3.

4.4. Gd(III) EPR spectra

The lanthanides in the 3+ oxidation state (except La and Lu) have unpaired f electrons, which make them paramagnetic. Some Ln(III) exhibit very large magnetic moments, μ_B . The Gd(III) ion, with a half-filled f-shell, has seven unpaired electrons ($S = 7/2$) which generate the largest magnetic moment and, thus, the highest paramagnetic character in the series. Gd(III), with a $4f^7$ electronic configuration ($^8S_{7/2}$), is the only trivalent lanthanide whose electron paramagnetic resonance (EPR) can be observed at room temperature. The Gd(III) ion is widely used as a probe to study the local environment of the host metal site in terms of symmetry and coordination in Gd salts. The EPR study of the Gd(III) ion concerned only metal salts in which Gd had been introduced as a dopant ($<1\%$) into crystals. It is also a very interesting problem to elucidate the role and nature of the 4f elements in coordination chemistry. We have used the EPR method to study pure gadolinium complexes [33,34]. Because of the strong spin–spin interactions the EPR spectra for such compounds are very broad and no details are observed. However, using computer processing (based on Fourier transform) we could enhance the spectral resolution to reveal the fine structure of the powder spectra of gadolinium β -diketonates [33] and polycarboxylates [34].

Polyoxometalates are purely inorganic compounds which offer attractive properties as Gd(III) ligands. In our studies the EPR spectra of Gd(III)–POM complexes, as polycrystalline powder, were measured and the effects of the coordinating ligands investigated [35,36]. The EPR spectra of Gd/POM, due to a smaller Gd(III) content in the POM composition, have much better resolution than others studied recently. In such cases the spin–spin interactions between ions are smaller and therefore the spectra are better resolved. The spectra of Gd(III)–POM, containing 1.7 to 2.5% Gd(III), do not require additional computer processing for correct interpretation. In the case of β -diketonates and polycarboxylates [with a Gd(III) content of 22–33%] it was necessary to use a computer program (based on Fourier transform) to enhance the spectral resolution.

The EPR spectra of Gd/POM allow us to observe the existence of the Gd(III) ion in two different surroundings: in a strong crystal field of rhombic symmetry and in a

Table 3
Infrared vibrational data for the FTIR spectra of selected heteropolytungstate anions^a

Heteropolytungstate anion	$\nu(\text{O-H})$ (cm^{-1})	$\delta(\text{O-H})$ (cm^{-1})	$\nu(\text{P-O}_a)$ or $\nu(\text{Si-O}_a)$ (cm^{-1})	$\nu(\text{W=O}_d)$ or $\nu(\text{Mo=O}_d)$ (cm^{-1})	(As-O _a) or (Sb-O) (cm^{-1})	$\nu(\text{W-O}_b\text{-W})$ (cm^{-1})	$\nu(\text{W-O}_c\text{-W})$ or $\nu(\text{Mo-O}_c\text{-Mo})$ (cm^{-1})
(SiW ₁₁ O ₃₉) ⁸⁻	3346.4s	1623.6s	980.6vw	935.3vw			725.6s 793.6
[Eu(SiW ₇ Mo ₄ O ₃₉) ₂] ¹³⁻	3546.3s	1616.4s	1004.2	940.8			720.5 761.6s 818.6
(P ₂ W ₁₈ O ₆₂) ⁶⁻	3481.4s 3567.3s	1612.2s	1020.2vw 1090.3s	958.7		911.3	776.4s
(P ₂ W ₁₇ O ₆₁) ¹⁰⁻	3447.0s 3522.4s	1616.3s	1016.0 1051.7 1083.9s	940.6s		889.3	733.8s 807.4s
[Eu(P ₂ W ₁₇ O ₆₁) ₂] ¹⁷⁻	3446.6s	1616.5s	1056.6 1085.1s	940.9s		889.0vw 919.4w	733.8 769.6s 824.2
(EuW ₁₀ O ₃₆) ⁹⁻	3447.1s	1652.7s		947.5		845.2	704.4s 783.8s
[(Na)As ₄ W ₄₀ O ₁₄₀] ²⁷⁻	3384.4	1616.8		949.9	794.3	877.2s	706.6s 628.2
[(Eu)As ₄ W ₄₀ O ₁₄₀] ²⁵⁻	3423.8s	1622.9s		956.4	784.0	850.4 883.2	703.9 628.7
[(Na)Sb ₉ W ₂₁ O ₈₆] ¹⁸⁻	3370.0vw 3520.0vw	1616.5w		916.1	770.5	825.2	695.0 739.0
[(Eu)Sb ₉ W ₂₁ O ₈₆] ¹⁶⁻	3362.3s	1623.6s		930.7	771.1	818.8 877.5w	699.0vw 734.7vw
[(Na)P ₅ W ₃₀ O ₁₁₀] ¹⁴⁻	3450.0s	1610.1s	1082.8 1163.7s	912.0 935.8			778.4s
[(Eu)P ₅ W ₃₀ O ₁₁₀] ¹²⁻	3450.0s	1610.2s	1019.5w 1066.8s 1161.9s	912.1 939.3			772.6s

^a vw, very weak; w, weak; s, strong.

weak crystal field. The symmetry of the gadolinium sandwiched complexes is probably lower than that of gadolinium-encapsulated complexes. This also means that the value of the zero-field splitting (ZFS) parameter (D) increases. In the case of [GdP₅W₃₀O₁₁₀]¹²⁻, the Gd(III) ion is unsymmetrically encapsulated with two (probably linearly bounded) water molecules and most likely the third water molecule has a different coordination environment [35]. The EPR spectrum of the [GdP₅W₃₀O₁₁₀]¹²⁻ complex showed the presence of lines characteristic for Gd(III) complexes having three water molecules in the inner coordination sphere and a line ($g = 2.65$) which is typically observed for complexes with two water molecules in the inner coordination sphere. We conclude that the third water molecule, due to an anisotropy effect, influences the EPR spectra of the [LnP₅W₃₀O₁₁₀]¹²⁻ complex, and is not directly encrypted [10,23,35], and is symmetry lowering [36]. The value of the zero-field splitting parameter D in the case of the

[Gd(SiW₁₁O₃₉)₂]¹³⁻ complex is ~ 1050 MHz, whereas in the case of the [GdP₅W₃₀O₁₁₀]¹²⁻ complex it is > 1150 MHz, with the effect of the crystal field more evident in the case of [GdP₅W₃₀O₁₁₀]¹²⁻. Complexation of Gd(III) by the lacunary ligand does not affect the complex structure and its symmetry as strongly as the gadolinium encapsulation process.

Acknowledgements

This work was supported by the Polish State Committee for Scientific Research, grant No. 3 T09A 106 14.

References

- [1] M.T. Pope, Heteropoly and Isopolyoxometalates, Springer, New York, 1983.

- [2] M.T. Pope, A. Muller (Eds.), *Polyoxometalates: From Platonic Solids to Anti-Retroviral Activity*, Kluwer Academic, Dordrecht, 1994.
- [3] J.T. Rhule, C.L. Hill, D.A. Judd, R.F. Schinazi, *Chem. Rev.* 98 (1) (1998) 327.
- [4] D.E. Katsoulis, *Chem. Rev.* 98 (1) (1998) 359.
- [5] M.T. Pope, B.W. Dale, *Q. Rev. Chem. Soc.* 22 (1968) 527.
- [6] M.T. Pope, *Inorg. Chem.* 11 (1972) 1973.
- [7] D.L. Kelpert, *Inorg. Chem.* 8 (1969) 1556.
- [8] C. Preyssler, *Bull. Soc. Chim. Fr.* 1 (1970) 30.
- [9] I. Creaser, M.C. Heckel, R.J. Neitz, M.T. Pope, *Inorg. Chem.* 32 (1993) 1573.
- [10] M.R. Antonio, L. Soderholm, *Inorg. Chem.* 33 (1994) 5988.
- [11] M.T. Pope, A. Muller, *Angew. Chem. Int. Ed. Engl.* 30 (1991) 34.
- [12] K. Nomiya, M. Miwa, *Polyhedron* 3 (1984) 341.
- [13] W.G. Klemperer, W. Shum, *J. Am. Chem. Soc.* 98 (1976) 829.
- [14] V.W. Day, W.G. Klemperer, *Science* 228 (1985) 4699.
- [15] T. Yamase, in: M.T. Pope, A. Muller (Eds.), *Polyoxometalates: From Platonic Solids to Anti-Retroviral Activity*, Kluwer Academic, Dordrecht, 1994, p. 337, and references therein.
- [16] C. Rocchiccioli-Deltcheff, M. Fournier, R. Franck, R. Thouvenot, *Inorg. Chem.* 22 (1983) 207.
- [17] A. Tézé, G. Hervé, *J. Inorg. Nucl. Chem.* 39 (1977) 999.
- [18] M.T. Pope, G.M. Varga, *Inorg. Chem.* 5 (1966) 1249.
- [19] M.A. Fernandez, G.J. Bastiaans, *Anal. Chem.* 51 (1979) 1402.
- [20] J. Aveston, *Inorg. Chem.* 3 (1964) 981.
- [21] K.Y. Matsumoto, Y. Sasaki, *Bull. Chem. Soc. Jpn.* 49 (1976) 156.
- [22] S. Lis, S. But, *J. Alloys Comp.* (in press).
- [23] S. Lis, M. Elbanowski, S. But, *Acta Phys. Pol. A* 90 (1996) 361.
- [24] W.T. Carnall, in: K.A. Gschneidner, L.R. Eyring (Eds.), *Handbook on the Physics and Chemistry of Rare Earths*, Vol. 3, North-Holland, Amsterdam, 1979, p. 171.
- [25] S. Lis, S. But, *J. Alloys Comp.* (in press).
- [26] K. Bukietynska, A. Mondry, *Inorg. Chim. Acta* 110 (1985) 1.
- [27] W. De W. Horrocks, D.R. Sudnick, *J. Am. Chem. Soc.* 101 (1979) 334.
- [28] P.P. Barthelemey, G.R. Choppin, *Inorg. Chem.* 23 (1989) 2044.
- [29] S. Lis, S. But, *Mater. Sci. Forum* 315–317 (1999) 431.
- [30] S. Lis, S. But, *J. Incl. Phenom. Mol. Recogn. Chem.* 35 (1999) 225.
- [31] G. Blasse, *Eur. J. Solid State Inorg. Chem.* 28 (1991) 719.
- [32] C. Rocchiccioli-Deltcheff, *Inorg. Chem.* 22 (1984) 207.
- [33] A. Szyzewski, R. Krzyminiewski, S. Lis, J. Pietrzak, M. Elbanowski, Z. Kruczynski, *J. Appl. Spectrosc.* 62 (1995) 165.
- [34] A. Szyzewski, R. Krzyminiewski, S. Lis, J. Pietrzak, M. Elbanowski, *Radiat. Phys. Chem.* 45 (1995) 935.
- [35] A. Szyzewski, S. Lis, Z. Kruczynski, J. Pietrzak, S. But, M. Elbanowski, *Acta Phys. Pol. A* 90 (1996) 275.
- [36] A. Szyzewski, S. Lis, Z. Kruczynski, S. But, J. Pietrzak, M. Elbanowski, *J. Alloys Comp.* 275–277 (1998) 349.